Discovery of FLT3 inhibitors for the treatment of acute myeloid leukemia

Grimm, S.H.

Cover Page

Universiteit Leiden

The handle http://hdl.handle.net/1887/68880 holds various files of this Leiden University dissertation.

Author: Grimm, S.H.
Title: Discovery of FLT3 inhibitors for the treatment of acute myeloid leukemia
Issue Date: 2019-02-20

Chapter 6

Summary and future prospects[*]

Chapter 1 introduces the scope and relevance of the research presented in this thesis. Starting at the question of what cancer is, how it evolves and how driver mutations can be used as a starting point for drug development. AML as well as FLT3 are introduced and current treatment and challenges thereof are outlined. Mapping cellular kinase inhibition profiles of clinical compounds is important to assess their off-target activity, but suitable methodology for this purpose is not available. **Chapter 2** describes the development of a label-free chemical proteomics based kinase selectivity assay. To this end the probe XO44 (Structure shown in Figure 1)[1] was used to investigate kinase inhibitor target landscape in live cells. This assay has been applied to evaluate five clinical FLT3 inhibitors in two cell lines. Many known targets of these inhibitors could be confirmed in a cellular environment, but also new, previously not reported targets could be identified, such as SRC, SLK and STK10 for gilteritinib. While this assay allows the evaluation of cellular selectivity for the first time, there are several opportunities for improvement. High concentrations of reversible kinase inhibitors are generally required to outcompete the covalent probe. When using cell lysate, competitive chemical proteomics experiments with non-covalent inhibitors and a covalent probe can be tightly controlled by varying concentrations and incubation times.[2] This is not as easily done in live cells, where inhibitors and probes have to cross the cell membrane, before they can interact with protein targets.
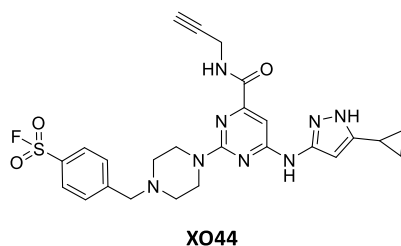

XO44

Figure 1: XO44, a chemical probe used for the proteomics based cellular selectivity assay used in chapter 2.

The sensitivity of the proteomics experiments can be improved by optimizing the peptide analysis and sample preparation methods. For example, chemical proteomics can be combined with whole genome sequencing. In the currently used bottom-up proteomics workflow, peptides are identified using MS/MS techniques and are further used to identify and quantify the proteins of the original sample. Since canonical proteome sequences are used small, non-functional differences in sequences could lead to substantial errors in identification and quantification of peptides, especially in cancer cells. With the continued decrease in costs in DNA sequencing, it becomes a viable option to combine whole genome sequencing with the chemical proteomics experiments, thereby ensuring that the identification and quantification algorithms work with the exact protein sequences present in the biological sample. Furthermore, potential post-translational modifications (PTMs) of the peptides should also be taken into account. This might be accomplished by simple treatment of a protein digest with broad-spectrum glycosidases, phosphatases and other PTM removing techniques.
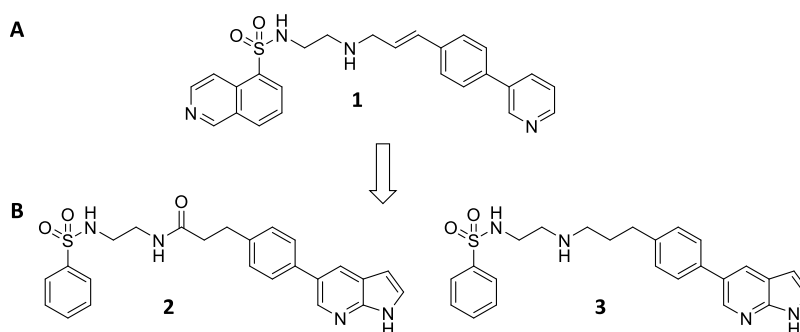

Figure 2: (A) The starting point of the structure-activity relationship study. (B) Two of the most active compounds discovered in the structure-activity relationship study of H-89 analogs as FLT3 inhibitors, described in chapter 3.

Chapter 3 describes the structure-activity relationship (SAR) of a H-89 derived chemical series as inhibitors for FLT3. During this effort several analogs were synthesized and tested against FLT3. Compound **1** was the starting point for this study (Figure 2A). Two of the most potent compounds (**2** and **3**) are shown in Figure 2B. The binding activity of these inhibitors could be substantially improved to picomolar inhibitors. Furthermore, the SAR indicated a surprising switch in binding mode, compared to the originally observed binding pose of H-89 in PKA. For example, the isoquinoline moiety, which interacts with amino acids in the hinge of PKA, was

dispensable for FLT3. Additional cellular assays with compounds **2** and **3** are required to assess their potential as leads for AML treatment. **Chapter 4** describes the search for FLT3 inhibitors with novel chemotypes that are active against drug-resistant FLT3 mutants. To this end a high throughput screen with a library of 231,152 compounds was performed. This led to the identification of 21 compounds, which were extensively profiled in various cellular assays to determine their effect of various FLT3 mutants. Two molecules, (Figure 3) were designated as suitable starting points for a hit optimization program.
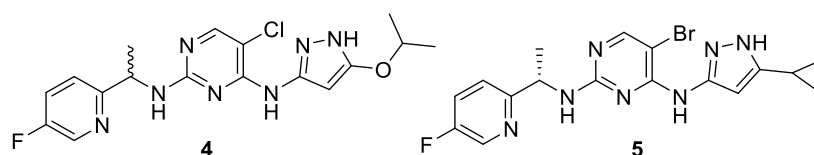

Figure 3: Structures of **4** (SPCE000476_01) and **5** (NP_004099_001), novel FLT3 inhibitors identified by HTS (Chapter 4).

Chapter 5 describes the optimization of compounds **4** and **5**. A number of compounds has been produced and biologically evaluated during this study. This efforts resulted in several cellular active, sub-nanomolar compounds with good molecular weight and lipophilicity. The structures of these compounds are shown in Figure 4 and they were further evaluated for their target profile in live cells using the chemical proteomics approach introduced in chapter 2. Subsequently these compounds were investigated in mice to evaluate their pharmacokinetic properties. Unfortunately, these studies showed that the compounds possessed poor oral bioavailability, which was due to a high intrinsic clearance. This is one of the main issues that need to be addressed for further development of these FLT3 inhibitors. This might be accomplished with either chemical of metabolic studies to identify the resulting metabolites and degradation hotspots. With this information structural changes can be introduced in the molecule to address to improve the chemical and metabolic stability.
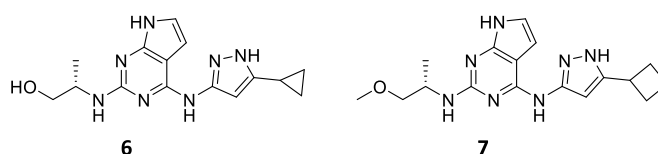

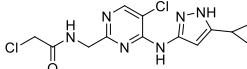Figure 4: Structure of optimized FLT3 inhibitors (Chapter 5).
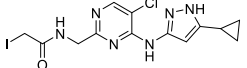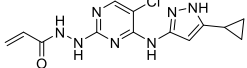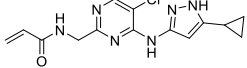
The future impact of small molecule FLT3 inhibitors on AML treatment will be revealed as more inhibitors with divers target profiles advance through clinical trials. The continued emergence of mutated AML cells in patients treated with FLT3 inhibitors also suggests that no single agent may be able to treat them all.[3,4] The optimal treatment will be chosen on the basis of the aberrant signaling pathways present in a patient. Further research is required to define the optimal therapy for each patient.

Another interesting approach is the development of covalent, irreversible inhibitors for FLT3, which may offer the possibility to have an alternative treatment strategy. Several covalent kinase inhibitors, targeting different kinases have been reported.[5] For example, ibrutinib and

acalabrutinib have been developed as covalent inhibitors for Bruton's tyrosine kinase (BTK) and are currently being used for the treatment of chronic lymphoma leukemias.[6–8]

To this end, covalent inhibitors for FLT3-ITD were designed. Structure-based studies suggested that cysteines (C694 and C828), located in the ATP-binding pocket of FLT3, could be targeted by electrophilic warheads introduced on the scaffold of compound **6**.[9] Subsequently, several inhibitors (compound **8** - **11**; Table 1) were synthesized and tested *in vitro*, as well as in the panel of cell lines. The results from this study are summarized in Table 1. Unfortunately, the compounds displayed submicromolar activity against recombinant enzyme and low activity against the cell lines. A potential reason for the low activity might either be a steric clash with the linker of the warhead or, alternatively, the replacement of the amine by an amide is not tolerated. In addition, the substitution of the amino-pyrimidine with the methyl-amino or hydrazine derivative might cause unfavorable electronic changes. Of note, different linkers or targeting C695, located outside the binding pocket, may provide alternative strategies to irreversibly inhibit FLT3.[10]

Table 1: Potential covalent FLT3 inhibitors.

| Entry | Structure | pIC$_{50}$ ± SEM | | | | | | | |
| | | *in vitro* FLT3 | MV4-11 | U937 | Ba/F3 | | | | |
					wt	FLT3 ITD	FLT3 ITD F691L	FLT3 ITD D835H	FLT3 ITD D835Y
8		6.39 ± 0.11	5.8 ± 0.2	< 5	< 5	5.4 ± 0.2	5.2 amb.	5.6 ± 0.2	5.6 ± 0.3
9		6.16 ± 0.13	6.5 ± 0.1	5.7 ± 0.2	5.5 ± 0.3	6.1 ± 0.1	6.0 amb.	6.0 ± 0.1	6.0 ± 0.1
10		6.05 ± 0.07	5.5 ± 0.1	ND	< 5	5.3 ± 0.1	< 5	5.2 ± 0.3	5.2 ± 0.1
11		6.58 ± 0.08	5.5 ± 0.1	ND	< 5	5.4 ± 0.2	5.0 ± 0.1	5.4 ± 0.3	5.6 ± 0.1

A novel strategy to indirectly disrupt FLT3 signaling is to inhibit ubiquitin carboxyl-terminal hydrolase 10 (USP10), the enzyme responsible for de-ubiquitination of FLT3. This will result in increased cellular degradation of FLT3 without the issue of the development of resistance conferring mutations in FLT3.[11]

The treatment of acute myeloid leukemia (AML) with mutated fms-like tyrosine kinase 3 (FLT3), especially internal tandem duplications in the juxtamembrane-domain (FLT3-ITD) remains a clinical challenge. The recent approval of midostaurin for FLT3-ITD in combination with cytarabine and daunorubicine benefits patients harboring FLT3 mutations.[12,13] The increase in 4-year overall survival rate from 44% (placebo treatment) to 51% (midostaurin

treatment) is, however, relatively modest. Furthermore, after remission patients are still advised to receive an allogenic bone marrow transplantation as a consolidation treatment.[14–16] AML is a genetically diverse disease with numerous mutations considered relevant for cancer progression (e. g. NPM1, CEBPA, RUNX1).[17–19] This exemplifies that FLT3 is not the only relevant drug target in AML as is also witnessed by the transient or incomplete clinical responses after FLT3-inhibitor monotherapy.[20] Thus, there remains an unmet medical need to discover new, additional therapies for FLT3-ITD AML patients.

In conclusion, the discovery of new FLT3 inhibitors is required to make AML a curable disease, but only in conjunction with other therapies. Determination of the cellular target interaction profile of kinase inhibitors will help to understand their impact on the complex signaling networks within cells. Chemical proteomics-based technologies, as developed in Chapter 2, can contribute to a better understanding of the molecular and cellular mode of action of drug candidates. Finally, novel and highly active molecules to inhibit FLT3 and its relevant mutations, such as described in this thesis, hold promise for future drug development efforts, especially when combined with other chemotherapies.

Experimental

Biochemical Evaluation of FLT3 inhibitors

In a 384-well plate (PerkinElmer 384 Flat White), 5 µL kinase/peptide mix (0.06 ng/µL FLT3 (Life Technologies; PV3182; Lot: 1614759F), 200 nM peptide (PerkinElmer; Lance® Ultra ULightTM TK-peptide; TRFO127-M; Lot: 2178856)) in assay buffer (50 mM HEPES (pH 7.5), 1 mM EGTA, 10 mM $MgCl_2$, 0.01% Tween-20, 2 mM DTT) was dispensed. Separately, inhibitor solutions (10 µM – 0.1 pM) were prepared in assay buffer containing 400 µM ATP and 1% DMSO. 5 µL of these solutions were dispensed and the plate was incubated for 90 minutes in the dark at room temperature. After 90 minutes the reaction was quenched by the addition of 10 µL of 20 mM EDTA containing 4 nM antibody (PerkinElmer; Lance® Eu-W1024-anti-phosphotyrosine(PT66); AD0068; Lot: 2342358). After mixing, samples were incubated for 60 minutes in the dark. The FRET fluorescence was measured on a Tecan Infinite M1000 Pro plate reader (excitation 320 nm, emission donor 615 nm, emission acceptor 665 nm). Data was processed using Microsoft Excel 2016, pIC_{50} values were fitted using GraphPad Prism 7.0. Final assay concentrations during reaction: 200 µM ATP, 0.03 ng/µL FLT3, 100 nM Lance TK-peptide, 0.5% DMSO. Compounds were tested in n=2 and N=2.

## In situ testing of kinase inhibitors

To evaluate inhibitor effect on cell proliferation MV4-11, U937 and Ba/F cell lines were grown in RPMI 10% fetal-bovine-serum. Ba/F cells (wild-type) are grown in the presence of IL-3 (10ng/ml, peprotech). All cells were cultured at 37°C under 5% CO_2. For viability assays, 10000 cells were seeded per well in a 96-wells plate and inhibitors were added at the indicated concentration. Three days later, cell viability was measured using the Cell Titer Blue viability assay (Promega), fluorescence was measured using the Clariostar (BMG Labtech). Relative survival was normalized to the untreated control and corrected for background signal.

Synthetic Procedures

Solvents were purchased from Biosolve, Sigma Aldrich or Fluka and, if necessary dried over 3Å or 4Å molecular sieves. Reagents purchased from chemical suppliers were used without further purification, unless stated otherwise. Oxygen or H_2O sensitive reactions were performed under argon or nitrogen atmosphere and/or under exclusion of H_2O. Microwave reactions were performed in a Biotage initiator+ microwave. Reactions were followed by thin layer chromatography analysis and was performed using TLC silica gel 60 F_{245} on aluminium sheets, supplied by Merck. Compounds were visualized by UV absorption (254 nm) or spray reagent (permanganate (5 g/L $KMnO_4$, 25 g/L K_2CO_3)). TLCMS was measured thin layer chromatography-mass spectrometer (Advion, EppressionL CMS; Advion, Plate Express). ^{1}H and ^{13}C-NMR spectra were performed on one of the following Bruker spectrometers: DPX 300 NMR spectrometer (300 MHz), equipped with 5mm-BBO-z-gradient-probe; AV-400 NMR spectrometer (400 MHz), equipped with 5mm-BBO-z-gradient-probe; AV-500 NMR spectrometer (500 MHz), equipped with BBFO-z-gradient-probe; AV-600 NMR spectrometer (600 MHz), equipped with 5mm-Cryo-z-gradient probe. NMR spectra were measured in deuterated methanol, chloroform or DMSO and were referenced to the residual protonated solvent signals as internal standards (chloroform-d = 7.260 (^{1}H), 77.160 (^{13}C); methanol-d_4 = 3.310 (^{1}H), 49.000 (^{13}C); DMSO-d_6 = 2.500 (^{1}H), 39.520 (^{13}C)). Signals multiplicities are written as s (singlet), bs (broad singlet), d (doublet), t (triplet), q (quartet), p (pentet) or m (multiplet). Coupling constants (J) are given in Hz. Preparative HPLC (Waters, 515 HPLC pump M; Waters,

515 HPLC pump L; Waters, 2767 sample manager; Waters SFO System Fluidics Organizer; Waters Acquity Ultra Performance LC, SQ Detector; Waters Binary Gradient Module) was performed on a Phenomenex Gemini column (5 µM C18, 150 x 4.6 mm) or a Waters XBridgeTM column (5 µM C18, 150 x 19 mm). Diode detection was done between 210 and 600 nm. Gradient: ACN in (H_2O + 0.2% TFA). HRMS (Thermo, Finnigan LTQ Orbitrap; Thermo, Finnigan LTQ Pump; Thermo, Finnigan Surveyor MS Pump PLUS Thermo, Finnigan Surveyor Autosampler; NESLAB, Merlin M25). Data acquired through direct injection of 1 mM of the sample in ACN/H_2O/t-BuOH (1:1:1), with mass spectrometer equipped with an electrospray ion source in positive mode (source voltage 3.5 kV, sheath gas low 10, capillary temperature 275°C) with resolution R = 60.000 at m/z = 400 (mass range = 150-2000) and dioctylphtalate (m/z = 391.28428) as lock mass. Gradient: ACN in (H_2O + 0.1% TFA). All tested compounds were checked for purity by LCMS liquid chromatography-mass spectrometer, a Thermo (Thermo Finnigan LCQ Advantage Max; Thermo Finnigan Surveyor LC-pump Plus; Thermo Finnigan Surveyor Autosampler Plus; Thermo Finnigan Surveyor PDA Plus Detector; Phenomenex Gemini column (5 µm C18, 50 x 4.6 mm)) system and were determined to be >95% pure by integrating UV intensity recorded.
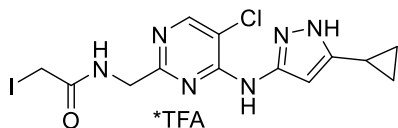
2-Chloro-*N*-((5-chloro-4-((5-cyclopropyl-1*H*-pyrazol-3-yl)amino)pyrimidin-2-yl)methyl)acetamide (8)
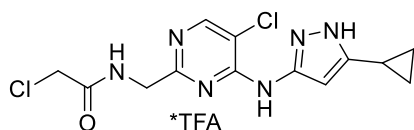
A flask was charged with HOBt (115 mg, 0.85 mmol, 1.13 eq), EDC (173 mg, 0.9 mmol, 1.2 eq) and 2-(aminomethyl)-5-chloro-*N*-(5-cyclopropyl-1*H*-pyrazol-3-yl)pyrimidin-4-amine (**14**) (198 mg, 0.75 mmol, 1 eq) suspended in THF (13.5 mL). The mixture was cooled down to 0°C and after addition of chloroacetic acid (82 mg, 0.87 mmol, 1.16 eq) the mixture was allowed to warm up and was stirred overnight at RT and concentrated under reduced pressure. The residue was purified via flash-column-chromatography (SiO$_2$, dry-loading, 10% (10% of sat. aqueous NH$_3$ in MeOH) in EtOAc) and preparative HPLC (Gemini C$_{18}$, 15% → 25% ACN in H$_2$O 0.2% TFA, 10 min gradient) to yield the compound as a TFA-salt after lyophilisation (209 mg, 61%). ^{1}H NMR (500 MHz, DMSO-d_6) δ 9.49 (s, 1H), 8.74 (t, J = 5.8 Hz, 1H), 8.42 (s, 1H), 6.36 (s, 1H), 4.35 (d, J = 5.9 Hz, 2H), 4.17 (s, 2H), 1.95 − 1.84 (m, 1H), 0.97 − 0.86 (m, 2H), 0.77 − 0.67 (m, 2H). ^{13}C NMR (126 MHz, DMSO-d_6) δ 166.55, 164.20, 155.40, 153.08, 147.15, 145.65, 112.56, 95.05, 44.75, 42.97, 8.18, 7.61. HRMS calculated for C$_{13}$H$_{15}$Cl$_2$N$_6$O 341.06789 [M+H]$^+$, found 341.0690. LCMS (ESI, C$_{18}$, linear gradient, 10% → 90% ACN in H$_2$O, 0.1% TFA, 10.5 min): t_R = 4.16 min; *m/z* : 341 [M+H]$^+$.

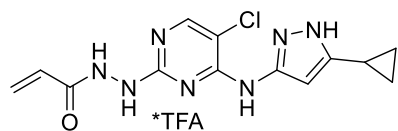### *N*-((5-Chloro-4-((5-cyclopropyl-1*H*-pyrazol-3-yl)amino)pyrimidin-2-yl)methyl)-2-iodoacetamide (9)

A flask was charged with HOBt (112 mg, 0.83 mmol, 1.11 eq), EDC (175 mg, 0.91 mmol, 1.22 eq) and 2-(aminomethyl)-5-chloro-*N*-(5-cyclopropyl-1*H*-pyrazol-3-yl)pyrimidin-4-amine (**14**) (198 mg, 0.75 mmol, 1 eq) suspended in THF (10 mL). The mixture was cooled down to 0°C and after addition of iodo acetic acid (156 mg, 0.84 mmol, 1.12 eq) the mixture was allowed to warm up and was stirred overnight at RT and concentrated under reduced pressure. The residue was purified via flash-column-chromatography (SiO$_2$, dry-loading, 10% (10% of sat. aqueous NH$_3$ in MeOH) in EtOAc) and preparative HPLC (Gemini C$_{18}$, 20% → 30% ACN in H$_2$O 0.2% TFA, 10 min gradient) to yield the compound as a TFA-salt after lyophilisation (153 mg, 37%). ^{1}H NMR (500

MHz, methanol-d_4) δ 8.32 (s, 1H), 6.38 (s, 1H), 4.45 (s, 2H), 3.83 (s, 2H), 2.01 – 1.90 (m, 1H), 1.05 – 0.97 (m, 2H), 0.85 – 0.72 (m, 2H). ^{13}C NMR (126 MHz, methanol-d_4) δ 169.96, 163.88, 155.49, 152.87, 148.41, 145.42, 112.77, 93.93, 44.85, 6.87, 6.77, -3.61. HRMS calculated for $C_{13}H_{15}ClIN_6O$ 433.00351 [M+H]$^+$, found 433.0047. LCMS (ESI, C_{18}, linear gradient, 10% → 90% ACN in H_2O, 0.1% TFA, 10.5 min): t_R = 4.31 min; m/z : 433 [M+H]$^+$.
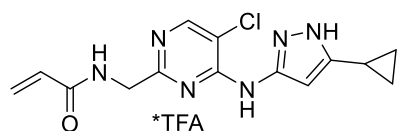
N'-(5-Chloro-4-((5-cyclopropyl-1*H*-pyrazol-3-yl)amino)pyrimidin-2-yl)acrylohydrazide (10)

A flask was charged with 5-chloro-*N*-(5-cyclopropyl-1*H*-pyrazol-3-yl)-2-hydrazineylpyrimidin-4-amine (**8**) (80 mg, 0.30 mmol, 1 eq) dissolved in DCM (5 mL) and DMF (2 mL). After the mixture was cooled to 0°C, EDC (51 mg, 0.36 mmol, 1.2 eq) and acrylic acid (30 µL, 0.45 mmol, 1.5 eq) were added and the mixture was allowed to warm up and stirred for 2 h at RT. The reaction was diluted with brine (10 mL) and extracted with EtOAc (3x10 mL). The combined organic layers were dried (Na₂SO₄), filtered and concentrated under reduced pressure to yield the di-substituted product. The residue was re-dissolved in 10% MeOH in H_2O and stirred overnight at RT. The reaction was diluted with DCM (20 mL), NaHCO₃ (20 mL) and brine (10 mL) and extracted with DCM (3x20 mL). The combined organic layers were washed with brine (2x20 mL), dried (Na₂SO₄), filtered and concentrated under reduced pressure. The residue was purified by preparative HPLC (Gemini C_{18}, 15% → 25% ACN in H_2O 0.2% TFA, 10 min gradient) to yield the compound as a TFA-salt after lyophilisation (1 mg, 1%). ^{1}H NMR (500 MHz, methanol-d_4) δ 8.03 (s, 1H), 6.44 – 6.29 (m, 3H), 5.84 (dd, *J* = 6.7, 5.3 Hz, 1H), 1.95 – 1.85 (m, 1H), 1.04 – 0.93 (m, 2H), 0.82 – 0.69 (m, 2H). HRMS calculated for $C_{13}H_{15}ClN_7O$ 320.10211 [M+H]$^+$, found 320.10218. LCMS (ESI, C_{18}, linear gradient, 0% → 50% ACN in H_2O, 0.1% TFA, 10.5 min): t_R = 5.62 min; m/z : 320 [M+H]$^+$.

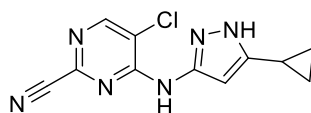### *N*-((5-Chloro-4-((5-cyclopropyl-1*H*-pyrazol-3-yl)amino)pyrimidin-2-yl)methyl) acrylamide (11)

A flask was charged with HOBt (50 mg, 0.372 mmol, 1.5 eq), EDC (65 mg, 0.421 mmol, 1.7 eq), acrylic acid (18 µL, 0.262 mmol, 1 eq) and 2-(aminomethyl)-5-chloro-*N*-(5-cyclopropyl-1*H*-pyrazol-3-yl)pyrimidin-4-amine (**7**) (67 mg, 0.252 mmol, 1 eq) suspended in DCM (6 mL). After addition of Et₃N (70 µL, 0.502 mmol, 2 eq) the mixture was stirred overnight, quenched with aqueous HCl (to pH ~6) and extracted with DCM (3x10 mL). the combined organic layers were washed with sat. aqueous NaHCO₃ (1x20 mL), brine (2x20 mL), dried (Na₂SO₄), filtered and concentrated under reduced pressure. The residue was purified by preparative HPLC (C_{18}, ACN in 50 mM NaHCO₃) to yield the compound after lyophilisation (15 mg, 19%). ^{1}H NMR (600 MHz, DMSO-d_6) δ 10.62 (s, 1H), 8.93 – 8.84 (m, 1H), 8.64 (s, 1H), 6.43 – 6.30 (m, 2H), 6.23 – 6.12 (m, 1H), 5.74 – 5.62 (m, 1H), 4.48 (d, *J* = 5.9 Hz, 2H), 1.97 – 1.85 (m, 1H), 1.04 – 0.92 (m, 2H), 0.85 – 0.71 (m, 2H). ^{13}C NMR (151 MHz, DMSO-d_6, 1% TFA) δ 165.45, 163.00, 155.43, 148.65, 148.15, 144.43, 131.25, 126.26, 112.35, 94.66, 42.98, 8.30, 7.11. HRMS calculated for $C_{14}H_{16}ClN_6O_3$ 319.10686 [M+H]$^+$, found 319.10699. LCMS (ESI, C_{18}, linear gradient, 0% → 50% ACN in H_2O, 0.1% TFA, 10.5 min): t_R = 5.81 min; m/z : 319 [M+H]$^+$.

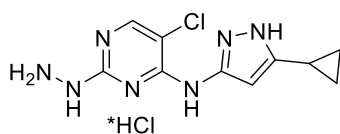### 2,5-Dichloro-*N*-(5-cyclopropyl-1*H*-pyrazol-3-yl)pyrimidin-4-amine (12)
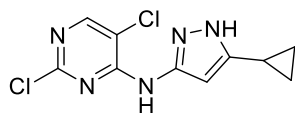
A round-bottom-flask was charged with 2,4,5-trichloropyrimidine (5.00 g, 27.26 mmol, 1 eq) dissolved in EtOH (35 mL). Et$_3$N (4.18 mL, 29.99 mmol, 1.1 eq) and 5-cyclopropyl-1*H*-pyrazol-3-amine (3.69 g, 29.99 mmol, 1.1 eq) dissolved in EtOH (35 mL) were added dropwise and the reaction mixture was stirred ON at RT until a colorless precipitate was formed. The formed precipitate was filtered off, washed with ice-cold EtOH and dried under reduced pressure to yield the product (7.40 g, quant.). ^{1}H NMR (400 MHz, DMSO-d_6) δ 12.37 (s, 1H), 9.70 (s, 1H), 8.32 (s, 1H), 6.19 (s, 1H), 2.03 – 1.80 (m, 1H), 1.04 – 0.87 (m, 2H), 0.81 – 0.60 (m, 2H). ^{13}C NMR (101 MHz, DMSO-d_6) δ 157.14, 156.97, 155.25, 145.99, 145.64, 113.26, 95.69, 7.92, 6.94. LCMS (ESI, C$_{18}$, linear gradient, 10% → 90% ACN in H$_2$O, 0.1% TFA, 10.5 min): t$_R$ = 5.66 min; *m/z* : 270 [M+H]$^+$.

5-Chloro-*N*-(5-cyclopropyl-1*H*-pyrazol-3-yl)-2-hydrazineylpyrimidin-4-amine (13)

A round-bottom-flask was charged with 2,5-dichloro-*N*-(5-cyclopropyl-1*H*-pyrazol-3-yl)pyrimidin-4-amine (**12**) (0.40 g, 1.47 mmol, 1 eq), DABCO (32 mg, 0.286 mmol, 0.2 eq) and NaCN (0.105 g, 2.14 mmol, 1.5 eq) dissolved in H$_2$O (3 mL) and DMSO (6 mL). The mixture was stirred for 5 h at 80°C before being diluted with EtOAc (75 mL) and H$_2$O (50 mL). The layers were separated and the aqueous layer was extracted with DCM (2x50 mL). The combined organic layers were washed with sat. aqueous NaHCO$_3$ (1x50 mL) and H$_2$O (1x50 mL), dried (Na$_2$SO$_4$), filtered, concentrated under reduced pressure and the ressidue purified via flash-column-chromatography (dry-loading, SiO$_2$, 40% → 70% EtOAc in pentane) to yield the product (322 mg, 84%). ^{1}H NMR (500 MHz, methanol-d_4) δ 8.42 (s, 1H), 6.32 (s, 1H), 1.95 (tt, *J* = 8.5, 5.1 Hz, 1H), 1.04 – 0.97 (m, 2H), 0.79 – 0.74 (m, 2H). ^{13}C NMR (126 MHz, methanol-d_4) δ 157.43, 155.00, 142.92, 118.89, 116.64, 95.99, 8.19, 7.74. LCMS (ESI, C$_{18}$, linear gradient, 10% → 90% ACN in H$_2$O, 0.1% TFA, 10.5 min): t$_R$ = 5.49 min; *m/z* : 261 [M+H]$^+$.

2-(Aminomethyl)-5-chloro-*N*-(5-cyclopropyl-1*H*-pyrazol-3-yl)pyrimidin-4-amine (14)
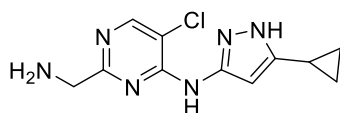
A flask was charged with 5-chloro-*N*-(5-cyclopropyl-1*H*-pyrazol-3-yl)-2-hydrazineylpyrimidin-4-amine (**13**) (0.32 g, 1.23 mmol, 1 eq) dissolved in MeOH (12 mL) and AcOH (1.3 mL). After addition of Pd/C (10%) the mixture was degassed and H$_2$ gas was bubbled through while sonicating for 20 min. The reaction was stirred for another 16 h under H$_2$ atmosphere. The resulting mixture was filtered over celite, concentrated under reduced pressure and purified via flash-column-chromatography (SiO$_2$, dry-loading, 10% → 40% (10% of sat. aqueous NH$_3$ in MeOH) in EtOAc) to yield the product (0.24 g, 71%). ^{1}H NMR (400 MHz, methanol-d_4) δ 8.29 (s, 1H), 6.33 (s, 1H), 3.84 (s, 2H), 1.99 – 1.88 (m, 1H), 1.08 – 0.93 (m, 2H), 0.83 – 0.70 (m, 2H). ^{13}C NMR (101 MHz, methanol-d_4) δ 168.56, 156.92, 154.32, 113.75, 95.26, 47.65, 8.24, 8.08. LCMS (ESI, C$_{18}$, linear gradient, 10% → 90% ACN in H$_2$O, 0.1% TFA, 10.5 min): t$_R$ = 1.01 min; *m/z* : 265 [M+H]$^+$.

5-Chloro-*N*-(5-cyclopropyl-1*H*-pyrazol-3-yl)-2-hydrazineylpyrimidin-4-amine (15)

A round-bottom-flask was charged with 2,5-dichloro-*N*-(5-cyclopropyl-1*H*-pyrazol-3-yl)pyrimidin-4-amine (**12**) (0.270 g, 1.0 mmol, 1 eq) dissolved in EtOH (5.3 mL). After addition of hydrazine monohydrate (0.152 mL, 3 mmol, 3 eq) the reaction was stirred at RT for 23 h. The formed product precipitated was

collected by filtration as a HCl salt (0.235 g, 78%). ^{1}H NMR (300 MHz, DMSO-d_6) δ 12.28 (s, 1H), 8.53 (s, 1H), 8.33 (s, 1H), 8.08 (s, 1H), 7.98 (s, 1H), 4.18 (s, 2H), 1.85 (m, 1H), 0.89 (m, 2H), 0.70 (m, 2H). ^{13}C NMR (75 MHz, DMSO-d_6, 1% TFA) δ 158.29, 155.43, 151.46, 147.45, 144.69, 106.06, 94.48, 8.01, 7.38. LCMS (ESI, C$_{18}$, linear gradient, 10% → 90% ACN in H$_2$O, 0.1% TFA, 10.5 min): t$_R$ = 0.72 min; *m/z* : 266 [M+H]$^{+}$.

References

(1)   Zhao, Q.; Ouyang, X.; Wan, X.; Gajiwala, K. S.; Kath, J. C.; Jones, L. H.; Burlingame, A. L.; Taunton, J. Broad-Spectrum Kinase Profiling in Live Cells with Lysine-Targeted Sulfonyl Fluoride Probes. *J. Am. Chem. Soc.* **2017**, *139* (2), 680–685.

(2)   Baggelaar, M. P.; Chameau, P. J. P.; Kantae, V.; Hummel, J.; Hsu, K.-L.; Janssen, F.; van der Wel, T.; Soethoudt, M.; Deng, H.; den Dulk, H.; et al. Highly Selective, Reversible Inhibitor Identified by Comparative Chemoproteomics Modulates Diacylglycerol Lipase Activity in Neurons. *J. Am. Chem. Soc.* **2015**, *137* (27), 8851–8857.

(3)   Man, C. H.; Fung, T. K.; Ho, C.; Han, H. H. C.; Chow, H. C. H.; Ma, A. C. H.; Choi, W. W. L.; Lok, S.; Cheung, A. M. S.; Eaves, C.; et al. Sorafenib Treatment of FLT3-ITD(+) Acute Myeloid Leukemia: Favorable Initial Outcome and Mechanisms of Subsequent Nonresponsiveness Associated with the Emergence of a D835 Mutation. *Blood* **2012**, *119* (22), 5133–5143.

(4)   Smith, C. C.; Lasater, E. a.; Zhu, X.; Lin, K. C.; Stewart, W. K.; Damon, L. E.; Salerno, S.; Shah, N. P. Activity of Ponatinib against Clinically-Relevant AC220-Resistant Kinase Domain Mutants of FLT3-ITD. *Blood* **2013**, *121* (16), 3165–3171.

(5)   Zhao, Z.; Bourne, P. E. Progress with Covalent Small-Molecule Kinase Inhibitors. *Drug Discov. Today* **2018**, *23* (3), 727–735.

(6)   Wu, J.; Zhang, M.; Liu, D. Acalabrutinib (ACP-196): A Selective Second-Generation BTK Inhibitor. *J. Hematol. Oncol.* **2016**, *9* (1), 21.

(7)   Byrd, J. C.; Harrington, B.; O'Brien, S.; Jones, J. A.; Schuh, A.; Devereux, S.; Chaves, J.; Wierda, W. G.; Awan, F. T.; Brown, J. R.; et al. Acalabrutinib (ACP-196) in Relapsed Chronic Lymphocytic Leukemia. *N. Engl. J. Med.* **2016**, *374* (4), 323–332.

(8)   Brown, J. R. Ibrutinib (PCI-32765), the First BTK (Bruton's Tyrosine Kinase) Inhibitor in Clinical Trials. *Curr. Hematol. Malig. Rep.* **2013**, *8* (1), 1–6.

(9)   Griffith, J.; Black, J.; Faerman, C.; Swenson, L.; Wynn, M.; Lu, F.; Lippke, J.; Saxena, K. The Structural Basis for Autoinhibition of FLT3 by the Juxtamembrane Domain. *Mol. Cell* **2004**, *13* (2), 169–178.

(10)   Yamaura, T.; Nakatani, T.; Uda, K.; Ogura, H.; Shin, W.; Kurokawa, N.; Saito, K.; Fujikawa, N.; Date, T.; Takasaki, M.; et al. A Novel Irreversible FLT3 Inhibitor, FF-10101, Shows Excellent Efficacy against AML Cells with FLT3 Mutations. *Blood* **2018**, *131* (4), 426–438.

(11)   Weisberg, E. L.; Schauer, N. J.; Yang, J.; Lamberto, I.; Doherty, L.; Bhatt, S.; Nonami, A.; Meng, C.; Letai, A.; Wright, R.; et al. Inhibition of USP10 Induces Degradation of Oncogenic FLT3. *Nat. Chem. Biol.* **2017**, *13* (12), 1207–1215.

(12)   Levis, M. Midostaurin Approved for FLT3-Mutated AML. *Blood* **2017**, *129* (26), 3403–3406.

(13)   Stone, R. M.; Mandrekar, S. J.; Sanford, B. L.; Laumann, K.; Geyer, S.; Bloomfield, C. D.; Thiede, C.; Prior, T. W.; Döhner, K.; Marcucci, G.; et al. Midostaurin plus Chemotherapy for Acute Myeloid Leukemia with a FLT3 Mutation. *N. Engl. J. Med.* **2017**, *377* (5), 454–

464.

(14)   Oran, B.; Cortes, J.; Beitinjaneh, A.; Chen, H.-C.; de Lima, M.; Patel, K.; Ravandi, F.; Wang, X.; Brandt, M.; Andersson, B. S.; et al. Allogeneic Transplantation in First Remission Improves Outcomes Irrespective of FLT3-ITD Allelic Ratio in FLT3-ITD–Positive Acute Myelogenous Leukemia. *Biol. Blood Marrow Transplant.* **2016**, *22* (7), 1218–1226.

(15)   Ho, A. D.; Schetelig, J.; Bochtler, T.; Schaich, M.; Schäfer-Eckart, K.; Hänel, M.; Rösler, W.; Einsele, H.; Kaufmann, M.; Serve, H.; et al. Allogeneic Stem Cell Transplantation Improves Survival in Patients with Acute Myeloid Leukemia Characterized by a High Allelic Ratio of Mutant FLT3-ITD. *Biol. Blood Marrow Transplant.* **2016**, *22* (3), 462–469.

(16)   Schechter, T.; Gassas, A.; Chen, H.; Pollard, J.; Meshinchi, S.; Zaidman, I.; Hitzler, J.; Abdelhaleem, M.; Ho, R.; Domm, J.; et al. The Outcome of Allogeneic Hematopoietic Cell Transplantation for Children with FMS-Like Tyrosine Kinase 3 Internal Tandem Duplication–Positive Acute Myelogenous Leukemia. *Biol. Blood Marrow Transplant.* **2015**, *21* (1), 172–175.

(17)   Welch, J. S.; Ley, T. J.; Link, D. C.; Miller, C. A.; Larson, D. E.; Koboldt, D. C.; Wartman, L. D.; Lamprecht, T. L.; Liu, F.; Xia, J.; et al. The Origin and Evolution of Mutations in Acute Myeloid Leukemia. *Cell* **2012**, *150* (2), 264–278.

(18)   Ding, L.; Ley, T. J.; Larson, D. E.; Miller, C. A.; Koboldt, D. C.; Welch, J. S.; Ritchey, J. K.; Young, M. A.; Lamprecht, T.; McLellan, M. D.; et al. Clonal Evolution in Relapsed Acute Myeloid Leukaemia Revealed by Whole-Genome Sequencing. *Nature* **2012**, *481* (7382), 506–510.

(19)   Döhner, H.; Weisdorf, D. J.; Bloomfield, C. D. Acute Myeloid Leukemia. *N. Engl. J. Med.* **2015**, *373* (12), 1136–1152.

(20)   Larrosa-Garcia, M.; Baer, M. R. FLT3 Inhibitors in Acute Myeloid Leukemia: Current Status and Future Directions. *Mol. Cancer Ther.* **2017**, *16* (6), 991–1001.